Direct inkjet printing of Si₃N₄: Characterization of ink, green bodies and microstructure

B. Cappi *, E. Özkol, J. Ebert, R. Telle

Department of Ceramics and Refractory Materials, RWTH Aachen University,
Mauerstrasse 5, D-52064 Aachen, Germany

Abstract

Direct inkjet printing of aqueous ceramic suspensions with high solid content was carried out for generating ceramic layers as well as 3D-components. In this study, silicon nitride (LPS-Si₃N₄) was suspended with organic additives in an aqueous medium. Subsequently the suspension was adapted to this manufacturing technique concerning particle size and deflocculation. Thin layers and micro-scaled 3D-components, e.g. gearwheels and engineering parts, were generated and pressureless sintered. Mechanical properties (fracture toughness K_{Ic}, hardness) and microstructure of printed LPS-Si₃N₄ were evaluated. Results show that dense structures with good mechanical properties were obtained. No delamination or other flaw-like textures were observed. The high potential for direct inkjet printing to manufacture high performance silicon nitride ceramics is thus demonstrated.
© 2008 Elsevier Ltd. All rights reserved.

1. Introduction

Silicon nitride (Si₃N₄) ceramics show excellent mechanical and thermal properties. For the densification of silicon nitride ceramics a liquid sintering mechanism is required due to the low self-diffusion coefficient and the tendency to evaporate. In the 1960s, dense ceramics were obtained providing an oxynitride liquid phase by the addition of various oxide and nitride additives in combination with hot-pressing.[1] Unfortunately, only simple geometries and shapes could be formed. In the following years, intensive research on Si₃N₄ resulted in the development of pressureless and gas pressure-aided sintering techniques, which made the production of complex shaped components possible.[2,3] In parallel, new shaping methods for technical ceramics were developed. Today various forming methods such as slip casting, tape casting, pressure injection moulding and cold-isostatic pressing followed by green machining are available.[4,5] These methods enable the production of components with complex geometries, but generally parts need further machining in order to fulfil the request for net shape contours.

Until presence, many so-called rapid manufacturing processes were developed for ceramics in order to manufacture customized parts without the expensive mechanical finishing: stereolithography (STL),[6–9] selective laser sintering (SLS),[10] fused deposition modeling (FDM), laminated object manufacturing (LOM), 3D-printing, multi-jet modeling,[6] and direct inkjet printing (DIP) have to be mentioned as the most important techniques. Among these, direct inkjet printing is a method for generating thin layers as well as micro-scaled 3D-components based on virtual models. In former studies, ceramic suspensions were used as inks for DIP and layers of oxide ceramics were generated. Aqueous ceramic suspensions of TiO₂, PbZr$_x$Ti$_y$O₃ and ZrO₂ were prepared and components containing textural defects were printed.[11–13] DIP of non-aqueous suspensions of TiO₂ [14,15] and ZrO₂ [16] was investigated too. The assembly of graduated components exemplified with ZrO₂, Al₂O₃, and carbon-based inks in order to achieve defined porosity[17,18] was carried out. Direct inkjet printing of aqueous suspensions was performed with ZrO₂ and dense structures were produced.[19] Thus, DIP demonstrates high potential to manufacture high performance ceramics. The goal of this study was to show the feasibility of direct inkjet printing of silicon nitride in aqueous medium and generate dense 3D-components.

---

* Corresponding author. Tel.: +49 241 8094985; fax: +49 241 8092226.
E-mail address: cappi@ghi.rwth-aachen.de (B. Cappi).

Table 1
Composition of the Si_3N_4 suspension

Material	Content (wt%)	Content (vol%)
Si_3N_4 powder	56.0	30.2
Yttium–aluminium–garnet powder	6.2	2.3
Distilled water	24.9	42.8
Ethylene glycol	4.4	6.8
Dispersant	0.2	0.3
Ethanol	7.2	15.7
Inorganic binder	0.7	1.1
Deflocculant	0.4	0.8

2. Experimental procedure

2.1. Materials

An α-Si_3N_4 powder (SN-E10, UBE Industries, Japan) with a specific surface area of $10\,m^2/g$ and a mean particle diameter of $0.5\,\mu m$ was used. An yttrium–aluminium–garnet powder (YAG, Sintertechnik, Pretzfeld, FRG) was added as sintering aid.

2.2. Preparation of the suspension

30.2 vol% Si_3N_4 and 2.3 vol% YAG were dispersed in aqueous medium using dispersants based on polyacrylic and carboxylic acid. The physical properties of the suspension were adjusted by addition of ethanol, ethylene glycol (Merck KGaA, Darmstadt, Germany), binder (PEG 400, Merck KGaA, Darmstadt, Germany) and an organic additive to avoid flocculation. The composition of the suspension is given in Table 1. The suspension was attrition milled using alumina balls as milling media. The particle size distribution was determined by laser-scattering (Mastersizer 2000, Malvern Instruments, UK). The viscosity of the suspension was measured at $20\,^{\circ}C$ using a rotating rheometer (Viscolab LC 10, Physica, Stuttgart, Germany).

2.3. Printing procedure

The printing system was a modified drop-on-demand HP DeskJet 930c. The printer has two separate cartridges for black and colour, each with an individual printhead working according to the bubble-jet principle.

The printing system was modified to enable layer-wise printing of cross-sections, drying and hardening the printed layers, and lowering the substrate to take up the next layer. The substrate position was controlled by a step motor. A printhead cleaning mechanism and a hardening unit were installed. Detailed information of the printing system is given in previous work.[19] A schematic view of the printing unit is shown in Fig. 1.

2.4. Sintering

The green bodies were debinded at $500\,^{\circ}C$ for 2 h. The printed samples were placed in a powder bed consisting of Si_3N_4, YAG and boron nitride in order to avoid decomposition of Si_3N_4. Pressureless sintering was carried out in a resistance heated fur-
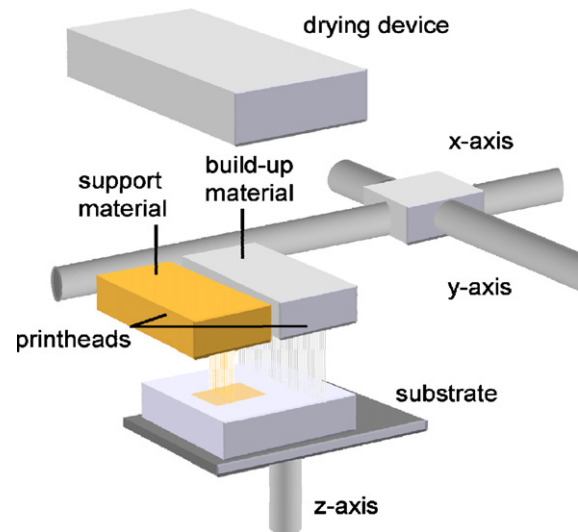

Fig. 1. The printing system[19].

nace (F 8127, FCT, Rauenstein, FRG) for 2 h at $1780\,^{\circ}C$ under 0.1 MPa flowing nitrogen atmosphere in a graphite die.

2.5. Material properties

Microstructure of green layers and sintered samples was characterized by SEM (Leo 440i, Leo Electron Microscopy, Cambridge, UK). The microstructure and the chemical composition of the sintered and plasma-etched surfaces were analyzed by SEM, TEM (CM 30, Philips, Eindhoven, NL) and EDX. Mineral phase analysis was performed using XRD (diffractometer PW 3710, Philips, Eindhoven, NL). The densities of the fired specimens were determined by the principle of Archimedes. Hardness was determined by Vickers indentation technique, fracture toughness (K_{Ic}) was calculated from median cracks emerging from the Vickers imprint according to the ICL-method.[20]

3. Results and discussion

Particle size distribution of the Si_3N_4 suspension is shown in Fig. 2. D_{50}-value after attrition milling was $0.4\,\mu m$. A stable and continuous printing process requires agglomerate sizes below $1\,\mu m$ to avoid mechanical clogging of the nozzles, which are approximately $30\,\mu m$ in diameter. Printing results show that both particle and agglomerate sizes were suitably adapted.
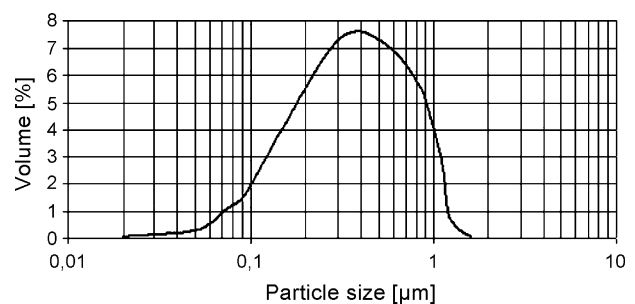

Fig. 2. Particle size distribution of the Si_3N_4 suspension.
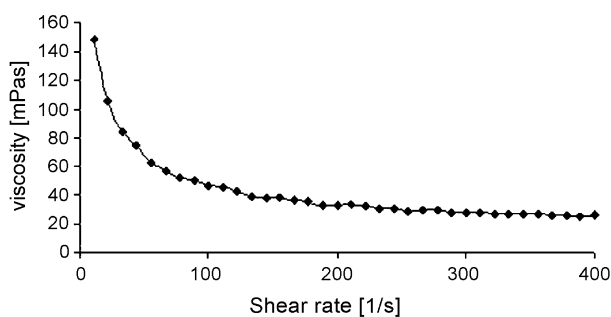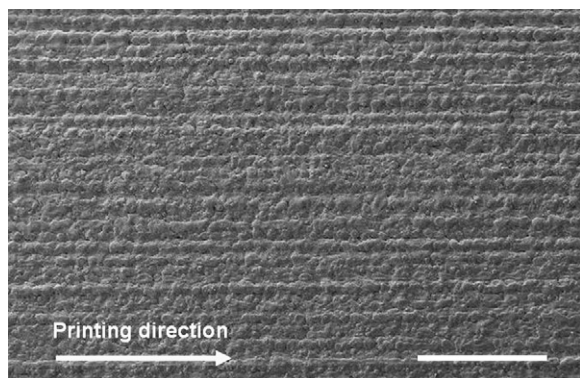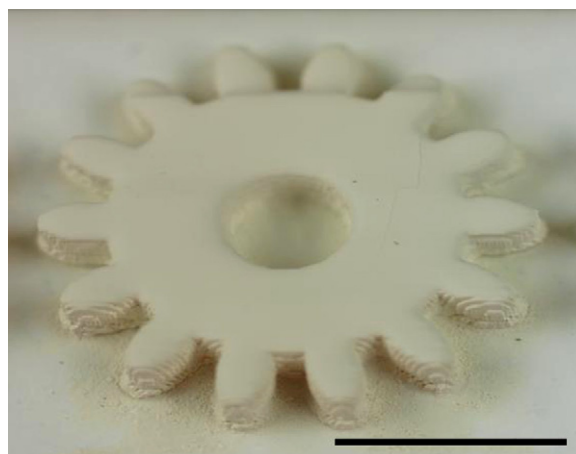
Fig. 3. Viscosity of the Si_3N_4 suspension.

Fig. 4. Surface of a green-printed layer, scale bar 1 mm.

The non-Newtonian flow behaviour of the Si_3N_4 suspension is shown in Fig. 3. At lower shear rates, shear forces have no effect on orientation of agglomerates and viscosity of the suspension is very high. At higher shear rates, viscosity decreases because of the disruption of the structures and the shear-induced orientation of Si_3N_4-particles. Hence, the suspension reveals shear thinning. No apparent changes in viscosity were observed at a shear rate of 250 1/s and above.

The surface of a green body consisting of 10 printed layers deposited upon each other is shown in Fig. 4. The printing direction is from left to right, horizontally arrayed droplet lines can be identified. The surface is homogenous and no process-dependent defects are visible. A high packing density of Si_3N_4 particles can be observed.

A gearwheel as an example of a technical part was printed and sintered afterwards. Fig. 5 shows a SEM-micrograph of the green gearwheel. The flaw-free surface of the sintered gearwheel and the accuracy of printing are shown in Fig. 6. The disproportionate outer contour of the cogs is due to deterioration of quality of data during the transformation from the 3D-file to the downscaled cross-sectional pictures to be printed. Hence, a better accuracy

Table 2
XRD-analysis of a printed Si_3N_4 specimen

Phase	Name
β-Si_3N_4	Silicon nitride
$Si_3Al_7O_3N_9$	Silicon oxynitride
Si	Silicon
$Y_4Si_3O_{12}$	Yttrium silicate

Fig. 5. Printed green Si_3N_4-gearwheel, scale bar 5 mm.

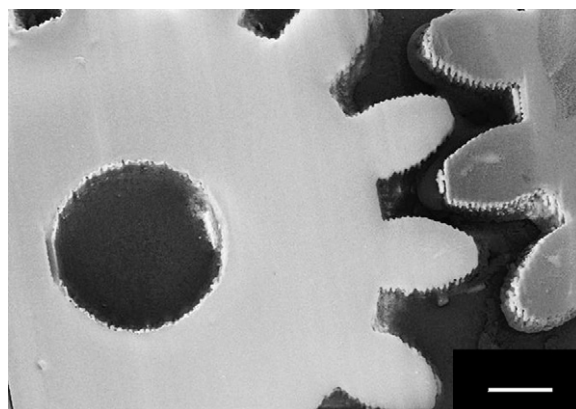of curved planes could be achieved by ensuring the original resolution.

Density of the sintered specimen was 3.18 g/cm^3. XRD analysis results are shown in Table 2. No α-Si_3N_4 was found in sintered specimen indicating that the transformation to β-Si_3N_4 was completed. The secondary phase consists of silicon oxynitride ($Si_3Al_7O_3N_9$), yttrium silicate ($Y_4Si_3O_{12}$) and a glassy phase. Traces of elemental silicon were found as well. It is assumed, that this is due to the decomposition of Si_3N_4 to Si and N_2 because of the pressureless sintering technique applied.

Figs. 7 and 8 show the microstructure of the sintered specimen. The microstructure is extremely homogenous. No printing defects, textures or other flaws caused by the printing process were detected by SEM and TEM. A homogeneous distribution of glassy phase is observed. The TEM-micrograph in Fig. 8 shows that the mean width of cross-section of the columnar β-Si_3N_4 crystals is around a value of 0.75 μm while the axial extension reaches 3 μm.

The material properties of sintered specimen are shown in Table 3. The fracture toughness K_{Ic} is with 4.4 MPam$^{0.5}$ comparatively low which is attributed to the small c/a ratio of the grains. A hardness value (HV 0.2) of 17 was achieved. Transverse rupture strength could not be determined because of the size and shape of the part. Because of the dense and homogeneous microstructure the mechanical properties of printed

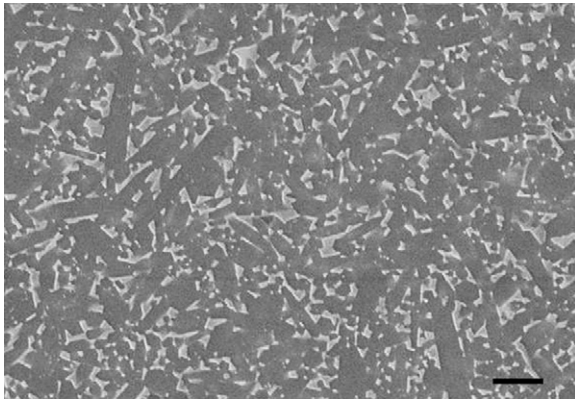Fig. 6. SEM-micrograph of sintered Si_3N_4-gearwheels, scale bar 1 mm.

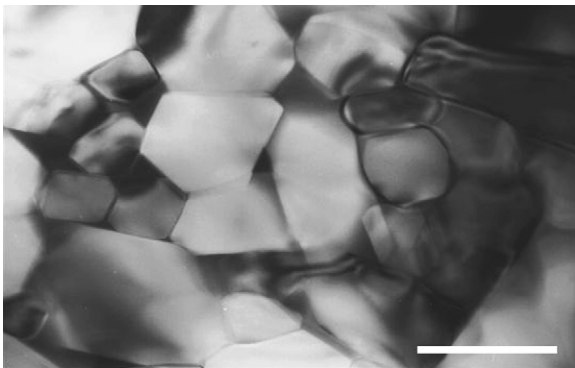Fig. 7. SEM-micrograph of the plasma-etched microstructure, scale bar 2 μm.

Fig. 8. TEM-micrograph of the microstructure, scale bar 400 nm.

Table 3
Material properties of sintered Si_3N_4 specimen

Material properties	Value
Density	3.18 g/cm^3
Mean grain size	0.75 μm (*a*-axis)
	3.0 μm (*c*-axis)
Hardness (HV 0.2)	17.0
Fracture toughness (K_{Ic})	4.4 MPam$^{0.5}$

test specimen show comparable values to those of dry pressed ones. Thus, a characteristic strength σ_0 of 600 MPa and above is expected which has to be proved by further investigations.

4. Conclusion

An aqueous Si_3N_4 suspension with a solid content of 30 vol% was prepared. Physical properties of the suspension were adjusted using organic and inorganic additives. Printing of layers and 3D-components was carried out with a printing system based on a commercially available office printer.

The following conclusions can be drawn:

(1) direct inkjet printing of dense non-oxide ceramics was successful. No lamination or other pecularities like textures were observed;
(2) promising mechanical properties were achieved;

(3) generation of parts with complex geometries is possible.

This study demonstrates the high potential of direct inkjet printing to manufacture high performance silicon nitride ceramics. For further investigations it is planned to produce a reliable number of test specimen via direct inkjet printing in order to analyse structural and mechanical properties of a series production, in particular 4-pt.-bending strength, Weibull modulus and Young's modulus. In parallel, the printing process is object of development to build up individually shaped engineering ceramic components.

Acknowledgement

References

1. Deeley, G. G., Herbert, J. M. and Moore, N. C., Dense silicon nitride. *Powder Metall.*, 1961, **8**, 145.
2. Terwilliger, G. R., Properties of sintered Si_3N_4. *J. Am. Ceram. Soc.*, 1974, **57**, 48.
3. Mitomo, M., Pressure sintering of Si_3N_4. *J. Mater. Sci.*, 1976, **11**, 1103.
4. Rabinovich, E. M., Leitner, S. and Goldenberg, A., Slip casting of silicon nitride for pressureless sintering. *J. Mater. Sci.*, 1982, **17**, 323–328.
5. Gutierrez, C. A. and Moreno, R., Tape casting of non-aqueous silicon nitride slips. *J. Am. Ceram. Soc.*, 2000, **20**, 1527–1537.
6. Chartier, T., Chaput, C., Doreau, F. and Louseau, M., Stereolithography of structural complex ceramic parts. *J. Mater. Sci.*, 2002(37), 3141–3147.
7. Doreau, F., Chaput, C. and Chartier, T., Stereolithography for manufacturing ceramic parts. *Adv. Eng. Mater.*, 2000, **2**(8), 493–496.
8. Leyland, N., Evans, J. and Harrison, D., Lithographic printing of ceramics. *J. Eur. Ceram. Soc.*, 2002, **22**, 1–13.
9. Licciulli, A., Corcione, C., Greco, A., Amicarelli, V. and Maffezzoli, A., Laser stereolithography of ZrO_2 toughened Al_2O_3. *J. Eur. Ceram. Soc.*, 2005, **25**, 1581–1589.
10. Lenk, R., Rapid prototyping of ceramic components. *Adv. Eng. Mater.*, 2000, **2**(1–2), 40–47.
11. Kim, S. and McKean, D., Aqueous TiO_2 suspension preparation and novel application of ink-jet printing technique for ceramics patterning. *J. Mater. Sci. Lett.*, 1998, **17**, 141–144.
12. Windle, J. and Derby, B., Ink jet printing of PZT aqueous ceramic suspensions. *J. Mater. Sci. Lett.*, 1999, **18**, 87–90.
13. Slade, C. and Evans, J., Freeforming ceramics using a thermal jet printer. *J. Mater. Sci. Lett.*, 1998, **17**, 1669–1671.
14. Blazdell, P., Evans, J., Edirisinghe, M., Shaw, P. and Binstead, M., The computer aided manufacture of ceramics using multilayer jet printing. *J. Mater. Sci. Lett.*, 1995, **14**, 1562–1565.
15. Blazdell, P. and Evans, J., Application of a continuous ink jet printer to solid freeforming of ceramics. *J. Mater. Process. Technol.*, 2000, **99**, 94–102.
16. Zhao, X., Evans, J. and Edirisinghe, M., Direct ink-jet printing of vertical walls. *J. Am. Ceram. Soc.*, 2002, **85**(8), 2113–2115.
17. Mott, M. and Evans, J., Zirconia/alumina functionally graded materials made by ceramic ink jet printing. *Mater. Sci. Eng.*, 1999, **A271**, 344–352.
18. Mott, M., Song, J.-H. and Evans, J., Microengineering of ceramics by direct ink-jet printing. *J. Am. Ceram. Soc.*, 1999, **82**(7), 1653–1658.
19. Ebert, J., Özkol, E., Telle, R., Fischer, H. and Uibel, K., Direct inkjet printing: a versatile method of complex shape manufacturing. In *Proceedings of the 10th European Ceramic Society Conference*, 2007.
20. Anstis, G. R., Chantikul, P., Lawn, B. R. and Marshall, D. B., A critical evaluation of indentation techniques for measuring fracture toughness. I. Direct crack measurements. *J. Am. Ceram. Soc.*, 1981, **64**(9), 533–538.